Perturbative approach to the nonequilibrium Kondo effect in a quantum dot

Tatsuya Fujii[1] and Kazuo Ueda[1,2]
[1]*Institute for Solid State Physics, University of Tokyo, Kashiwa 277-8581, Japan*
[2]*Advanced Science Research Center, Japan Atomic Energy Research Institute, Tokai 319-1195, Japan*
(Received 16 June 2003; published 15 October 2003)

The theory of quantum transport through a dot under a finite bias voltage is developed using perturbation theory in the Keldysh formalism. It is found that the Kondo resonance splits into double peaks when the voltage exceeds the Kondo temperature, $eV > k_B T_K$, which leads to the appearance of a second peak in conductance, in addition to the zero-bias peak. The possible relevance of the new peak to the 0.7 conductance anomaly observed in quantum point contact is discussed.

DOI: 10.1103/PhysRevB.68.155310 PACS number(s): 73.63.Kv, 72.15.Qm

I. INTRODUCTION

Ten years after the theoretical predictions of the Kondo effect in a quantum dot,[1,2] the zero-bias peak of the differential conductance was identified as the Kondo resonance.[3,4] The observation that the peak value reached the unitary limit of $2e^2/h$ with decreasing temperature established unambiguously that the Kondo effect is relevant to the transport properties of the quantum dot.[5] Clearly the new feature of Kondo transport compared with the usual Kondo effect of magnetic impurities is the nonequilibrium nature, since the current is measured with a finite bias voltage. Only in the limit of zero-bias voltage is the equilibrium condition recovered.

This theoretical study of the nonequilibrium Kondo effect is based on the Keldysh formalism.[6] In order to treat the correlation effect various methods have been used: one is perturbation theory with respect to the Coulomb interaction U in the dot,[7] and another often used method is the noncrossing approximation (NCA) where an infinite U is assumed.[8] Concerning the equilibrium Kondo problem, it is well known that second order perturbation theory gives remarkably good results.[9] For example, the density of states with the Kondo resonance in the middle of the side peaks corresponding to the energy levels in the atomic limit is well described by the theory. However, it is not clear whether second order perturbation theory works well in nonequilibrium conditions. On the other hand, concerning the NCA, it is well known that the analyticity is broken in the low temperature limit. Thus one cannot discuss the conductance in the unitary limit using the NCA.

One important theoretical issue is that the above mentioned theories predict contradictory results for the density of states (DOS) in the nonequilibrium case. The NCA predicts a splitting of the Kondo resonance under a finite bias voltage. On the other hand, in second order perturbation theory, the Kondo resonance peak is simply suppressed and does not show any particular structure in the nonequilibrium situation. Since the Kondo resonance is a manifestation of singlet formation between the localized state and the leads, it seems that the double peak structure at chemical potentials of both leads is reasonable. Indeed, the double peaks are also obtained by other approaches: equations of motion,[8,9] a real-time diagrammatic formulation,[10] and scaling methods.[11] Moreover, it is not clear how the effects of the double peak structure, if it is present, would appear in the differential conductance. Recently, a proposal was made to measure the splitting of the DOS by using three-terminal quantum dots.[12,13] As a matter of fact, the splitting of the Kondo peak was successfully observed by introducing a potential difference in the source lead.[14] This result is most likely due to the splitting of the Kondo resonance, although the precise geometry is different from the present case where a finite voltage is applied between the source and drain. It is clearly necessary to study nonequilibrium Kondo effects by a better theoretical approach.

In this paper we analyze the Kondo effect in a quantum dot with a finite voltage by using perturbation theory up to fourth order in U based on the Keldysh formalism. We show that with increasing bias voltage a single Kondo peak splits into double peaks at $eV \sim k_B T_K$. As a result, an anomalous peak of the differential conductance appears when $eV > k_B T_K$. At the end of this paper, we will also discuss the possible relevance to the experiments referred to as the 0.7 conductance anomaly in quantum point contacts (QPCs).[15–17]

II. MODEL AND CALCULATIONS

We consider a single-level quantum dot attached to two leads. This system is described by the Anderson impurity model,

$$H = \sum_{k\alpha\sigma} \varepsilon_{k\alpha} c^\dagger_{k\alpha\sigma} c_{k\alpha\sigma} + \sum_\sigma \epsilon_d n_\sigma + U n_\uparrow n_\downarrow + \sum_{k\alpha\sigma} (V_{k\alpha\sigma} c^\dagger_{k\alpha\sigma} d_\sigma + \text{H.c.}), \tag{1}$$

where $\alpha = L$ and R, and $c_{kL\sigma}$ ($c_{kR\sigma}$) annihilates an electron in the left (right) lead, d_σ annihilates an electron with spin σ in the dot, and $n_\sigma = d^\dagger_\sigma d_\sigma$. The coupling constants $V_{k\alpha\sigma}$ describe the tunneling matrix elements between the dot and leads. The nonequilibrium situation is driven by a finite difference between μ_L and μ_R which are the chemical potentials of the leads in both sides.

For simplicity we concentrate on the symmetric Anderson model, where the dot is symmetrically coupled with the leads and the energy level of the dot, including the Hartree mean

field $U\overline{n_\sigma}$, coincides with the center of the potential drop, $eV=\mu_L-\mu_R$. Then the symmetric conditions are stated as $\Gamma_{L\sigma}=\Gamma_{R\sigma}\equiv\Gamma$, $\mu_L=-\mu_R=eV/2$, and $-\epsilon_d=\epsilon_d+U$. Here $\Gamma_{L,R\sigma}$ represents the resonance width at the chemical potentials, $\Gamma_{L,R\sigma}(\omega)=2\pi\Sigma_k|V_{kL,R\sigma}|^2\delta(\omega-\varepsilon_{kL,R})$. In this paper we restrict ourselves to the ground state, $T=0$.

Our first aim is to calculate the density of states in the dot,

$$\rho_\sigma(\omega)=-\frac{1}{\pi}\mathrm{Im}G^r_\sigma(\omega), \tag{2}$$

where $G^r_\sigma(\omega)$ is the retarded Green function. Then the current through the dot is expressed by

$$I=\frac{e}{\hbar}\sum_\sigma\int_{-\infty}^{\infty}d\omega\frac{\Gamma_{L\sigma}\Gamma_{R\sigma}}{\Gamma_{L\sigma}+\Gamma_{R\sigma}}\rho_\sigma(\omega)[f_L(\omega)-f_R(\omega)], \tag{3}$$

where $f_{L,R}(\omega)=\theta(\mu_{L,R}-\omega)$. The differential conductance is obtained from the current by

$$G(V)=\frac{\partial I}{\partial V}. \tag{4}$$

III. KELDYSH FORMALISM

A. Perturbation theory

Now we briefly sketch the perturbation theory based on the Keldysh formalism.[6] Each of the terms generated by the expansion of the S matrix includes integrals along the Keldysh contour, which starts at $t=-\infty$, passes through $t=\infty$, and returns to $t=-\infty$. The branch from $t=-\infty$ ($t=\infty$) to $t=\infty$ ($t=-\infty$) is denoted by the index $-(+)$. Thus we need to introduce four types of Green functions with these additional indices $G^{\alpha\beta}$ where α and β are $-$ or $+$.

The interaction terms in the S matrix are given by the sum of the Coulomb interaction U at the dot and the hybridizations $V_{kL,R\sigma}$ between the leads and the dot. We employ a perturbation theory in U based on the Keldysh formalism where the Green functions in each order of U are renormalized by $V_{kL,R\sigma}$.

The Green functions of zeroth order in U can be explicitly evaluated as

$$g^{0-+}_\sigma(\omega)=-i|g^{0r}_\sigma(\omega)|^2\sum_{p=L,R}\Gamma_{p\sigma}(\omega)f_p(\omega), \tag{5}$$

$$g^{0+-}_\sigma(\omega)=+i|g^{0r}_\sigma(\omega)|^2\sum_{p=L,R}\Gamma_{p\sigma}(\omega)[1-f_p(\omega)] \tag{6}$$

by solving the Dyson equations concerning $V_{kL,R\sigma}$, where $g^{0r}_\sigma(\omega)=(\omega-\epsilon_d+i/2\cdot[\Gamma_{L\sigma}(\omega)+\Gamma_{R\sigma}(\omega)])^{-1}$. In order to estimate the diagonal components, it is more convenient to find the Fourier transform of

$$g^{0\alpha\alpha}_\sigma(t)=\theta(-\alpha t)g^{0+-}_\sigma(t)+\theta(\alpha t)g^{0-+}_\sigma(t), \tag{7}$$

rather than to solve $g^{0\alpha\alpha}_\sigma$ directly.

In the expansion in U there are diagrams in which Hartree type self-energies are inserted. Their contributions are entirely taken into account by substituting $\epsilon_d\to\epsilon_d+U\overline{n_{-\sigma}}$ in $g^{0\alpha\beta}_\sigma$ in the diagrams where the Hartree type of self-energies are omitted. Using $\epsilon_d+U\overline{n_{-\sigma}}=0$ for the symmetric case, the new Green functions $g^{\alpha\beta}_\sigma$ are

$$g^{-+}_\sigma(\omega)=-i2\,\mathrm{Im}g^r_\sigma(\omega)f_{\mathrm{eff}}(\omega), \tag{8}$$

$$g^{+-}_\sigma(\omega)=+i2\,\mathrm{Im}g^r_\sigma(\omega)[1-f_{\mathrm{eff}}(\omega)], \tag{9}$$

$$g^{--}_\sigma(\omega)=\frac{1-f_{\mathrm{eff}}(\omega)}{\omega+i\Gamma}+\frac{f_{\mathrm{eff}}(\omega)}{\omega-i\Gamma}, \tag{10}$$

$$g^{++}_\sigma(\omega)=-g^{--}_\sigma(\omega)^*, \tag{11}$$

where $\Gamma_{L,R\sigma}(\omega)$ approximated the values at the chemical potentials, $f_{\mathrm{eff}}(\omega)=(\Gamma_{L\sigma}f_L(\omega)+\Gamma_{R\sigma}f_R(\omega))/(\Gamma_{L\sigma}+\Gamma_{R\sigma})$ and $g^r_\sigma(\omega)=(\omega+i\Gamma)^{-1}$.

Then the Dyson equations for U may be written in matrix form,

$$G^{\alpha\beta}_\sigma(\omega)=g^{\alpha\beta}_\sigma(\omega)+g^{\alpha\gamma}_\sigma(\omega)\Sigma^{\gamma\delta}_\sigma(\omega)G^{\delta\beta}_\sigma(\omega). \tag{12}$$

Here in each order of $\Sigma^{\gamma_1\gamma_2}_\sigma$ it is sufficient to exclude Hartree type self-energies.

Let us evaluate the self-energies by using perturbation theory up to the fourth order of U. It is known that the perturbative expansion for the Anderson model[9] is effective and well behaved in the equilibrium case, since the exact solution shows a rapid convergence of the perturbation series.[18] However, in the nonequilibrium situation, the analysis of perturbation theory has been limited to second lowest order. To proceed to higher order calculations, the four-point vertex, which is obtained by extending the method used by Keldysh for the electron-phonon vertex,[6] is very convenient. This procedure is to insert vertices,

$$\Gamma^{(0)\alpha_1\alpha_2,\alpha_3\alpha_4}=U(\gamma^-_{\alpha_1\alpha_2}\gamma^-_{\alpha_3\alpha_4}-\gamma^+_{\alpha_1\alpha_2}\gamma^+_{\alpha_3\alpha_4}), \tag{13}$$

in each of diagrams, which may be called *the Keldysh vertices*. Here $\gamma^{\alpha_3}_{\alpha_1\alpha_2}=\delta_{\alpha_1\alpha_2}\sigma^z_{\alpha_2\alpha_3}$, where $\sigma^z_{\alpha_2\alpha_3}$ is the third Pauli matrix. All diagrams up to fourth order are shown in Fig. 1 for the symmetric case, where the third-order terms vanish in the same way as the equilibrium case. Figure 1(a) is the second order diagram in which directions of particle lines, spins, and Keldysh vertices are depicted. In this case, the second order correction of the self-energies is

$$\begin{aligned}\Sigma^{(2)\gamma_7\gamma_2}_\sigma(\omega)&=i^2(-1)\int_{-\infty}^{\infty}\frac{d\omega_1}{2\pi}\frac{d\omega_2}{2\pi}\Gamma^{(0)\gamma_1\gamma_2,\gamma_3\gamma_4}g^{\gamma_5\gamma_4}_\sigma\\&\quad\times(\omega_1)g^{\gamma_6\gamma_3}_{-\sigma}(\omega_2)g^{\gamma_1\gamma_8}_{-\sigma}(\omega_1+\omega_2-\omega)\Gamma^{(0)\gamma_5\gamma_6,\gamma_7\gamma_8}.\end{aligned} \tag{14}$$

We can proceed in the same way to the fourth order diagrams shown in Fig. 1(b). Four different representative diagrams are illustrated where directions and spin variable are not specified. By specifying them, one can immediately ob-

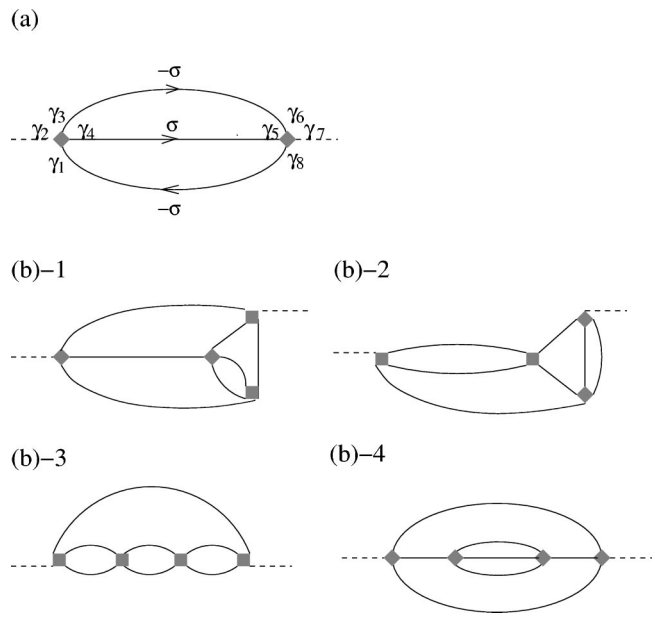

FIG. 1. (a) The second order diagram and (b) the fourth order diagrams. In (b) all 12 diagrams are generated by including the directions of particle lines and spins. Shaded squares represent the Keldysh vertices.

tain all 12 diagrams. Note that Fig. 1(b)-1,2,3 and Fig. 1(b)-4 are skeleton and nonskeleton diagrams, respectively. It is tedious but straightforward to evaluate the fourth order contributions, $\Sigma_\sigma^{(4)\gamma_1\gamma_2}$, in the same manner as the second order.

From the self-energy matrix, the imaginary part of Σ_σ^r is defined by

$$\mathrm{Im}\Sigma_\sigma^r(\omega)=\frac{1}{2}[i\Sigma_\sigma^{+-}(\omega)-i\Sigma_\sigma^{-+}(\omega)]. \tag{15}$$

Then the real part of Σ_σ^r is obtained by the Kramers-Kronig relation,

$$\mathrm{Re}\Sigma_\sigma^r(\omega)=\frac{1}{\pi}\mathcal{P}\int_{-\infty}^{\infty}\frac{\mathrm{Im}\Sigma_\sigma^r(\omega')}{\omega'-\omega}d\omega'. \tag{16}$$

The Dyson equation for the retarded component is derived from Eq. (12) as

$$G_\sigma^r(\omega)=g_\sigma^r(\omega)+g_\sigma^r(\omega)\Sigma_\sigma^r(\omega)G_\sigma^r(\omega). \tag{17}$$

B. Self-energies

In Fig. 2 the numerically calculated $\mathrm{Im}\Sigma_\sigma^r(\omega)$ is shown for $U/\Gamma=6$. In the equilibrium case of $eV/\Gamma=0$, $\mathrm{Im}\Sigma_\sigma^r|_{eV/\Gamma=0}$ is dominated by the second order contribution as is well known,[9] since the fourth order contributions of skeleton diagrams shown in Fig. 1(b)-1,2,3 and nonskeleton diagram in Fig. 1(b)-4 almost cancel each other except in the low energy limit. In order to analyze $\omega\sim 0$, it should first be noted that the present perturbation results correctly reproduce the low-energy asymptotic form in the equilibrium limit:[9]

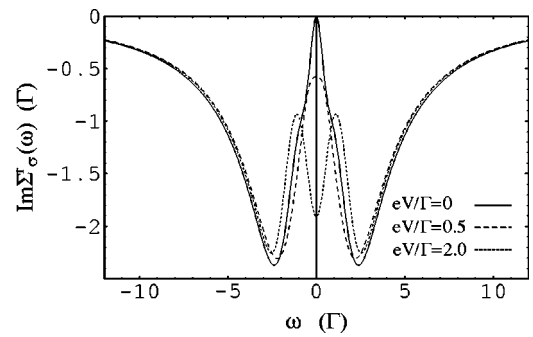

FIG. 2. The numerically calculated $\mathrm{Im}\Sigma_\sigma^r$ as a function of ω for $eV/\Gamma=0$, 0.5, and 2.0. In this example, U/Γ is 6.

$$\mathrm{Im}\Sigma_\sigma^r(\omega)|_{eV/\Gamma=0}\simeq\frac{\Gamma}{2}\left\{-\left(\frac{U}{\pi\Gamma}\right)^2-3(10-\pi^2)\left(\frac{U}{\pi\Gamma}\right)^4\right\}\times\left(\frac{\omega}{\Gamma}\right)^2.$$

The nonskeleton diagram does not give any contribution to the fourth order term of the coefficient of $(\omega/\Gamma)^2$. Among the skeleton diagrams of the random phase approximately (RPA)-type diagrams, Fig. 1(b)-3, give (-3×3) for the coefficient of $(U/\pi\Gamma)^4$, while those from the vertex-correction type, Fig. 1(b)-1 and 2, give $3\times(\pi^2-7)$, resulting in the small number of $-3\times(10-\pi^2)$. The way that cancellation occurs between the RPA-type diagrams and the vertex-correction-type diagrams changes under a finite bias voltage.

In the vicinity of the equilibrium (for example at $eV/\Gamma=0.5$), $-\mathrm{Im}\Sigma_\sigma^r(\omega=0)$ becomes slightly larger but still keeps the structure of the equilibrium case, which means that damping of quasiparticles is simply enhanced by real transitions between the leads and the dot. Novel features are observed with further increasing the voltage. The fourth order contribution to the coefficient of the $(\omega/\Gamma)^2$ term changes sign. Even though the second order contribution remains negative, the coefficient of $(\omega/\Gamma)^2$ becomes positive for sufficiently large $U/\pi\Gamma$. Therefore, the peak of $\mathrm{Im}\Sigma_\sigma^r$ around $\omega\sim 0$ becomes depressed. In this case the quasiparticles remain coherent around $\omega=\pm eV/2$ as is shown for $eV/\Gamma=2.0$

Now we turn to $\mathrm{Re}\Sigma_\sigma^r$ which is shown in Fig. 3. In the case of $eV/\Gamma=2.0$ we see the development of new zero

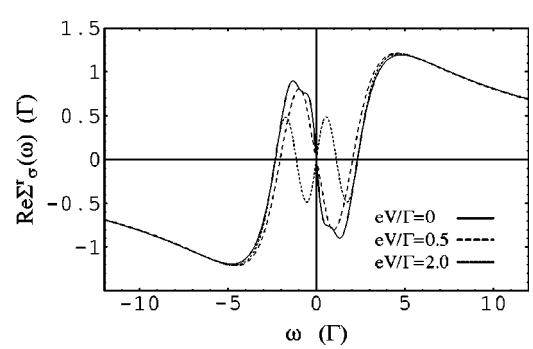

FIG. 3. The real part of the self-energy for $eV/\Gamma=0$, 0.5, and 2.0, with $U/\Gamma=6$.

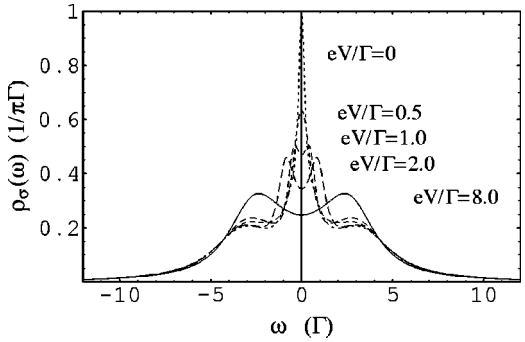

FIG. 4. The density of states in units of $1/\pi\Gamma$ for various eV/Γ with $U/\Gamma=6$.

points of $\mathrm{Re}\Sigma_\sigma^r$ at $\omega=\pm eV/2$ which are absent for $eV/\Gamma=0$ and 0.5. Since the slopes at the zero points are negative, which leads to mass enhancement, the effect of damping due to $\mathrm{Im}\Sigma_\sigma^r$, is reduced.

C. Density of states

The density of states is shown in Fig. 4 in units of $1/\pi\Gamma$. In the equilibrium case, the sharp Kondo peak develops in the middle of the two peaks at around $\pm U/2$. With a finite voltage, the Kondo peak at $\omega/\Gamma=0$ is suppressed but still keeps a *single* peak with broadening for small eV/Γ, in accordance with the analysis based on the Ward identities.[19] When the voltage is further increased, the Kondo peak splits into *double* peaks at $\omega\sim\pm eV/2$, which are located near the chemical potentials of the two leads. This behavior is qualitatively consistent with the results obtained by the NCA.[8] This change occurs when the potential drop eV exceeds k_BT_K, defined as the full width at half maximum of the Kondo peak. For $U/\Gamma=6$, k_BT_K/Γ is estimated to be about 0.6.

With higher bias the *double* Kondo peaks located at $\omega\sim\pm eV/2$ merge with the peaks at the atomic limit $\omega\sim\pm U/2$ and then the latter dominate when $eV>U$. We have checked that this structure coincides with the result obtained by the second order perturbation theory. The origin of this phenomena is that the higher order scatterings become unimportant in the high voltage regime due to the strong dissipative processes between the leads and the dot. This result is consistent with Ref. 11 in that the nonequilibrium decoherence destroys the Kondo effect when $eV\gg k_BT_K$.

IV. CONDUCTANCE

In Fig. 5 the differential conductance defined by Eq. (4) is shown in units of $2e^2/h$ for various values of U/Γ as a function of bias voltage. For all U, the zero-bias peak starts from the unitary limit. As U is increased, the width of the zero-bias peak becomes narrower. For $U/\Gamma=4$ and 6, a broad peak is seen at around $eV\sim U$. This broad peak corresponds to tunneling processes through the energy levels in the atomic limit. Between the zero-bias peak and the broad peak, a new peak appears for large U ($U/\Gamma=6$ in the figure).

To understand the origin of the new peak, first we rewrite

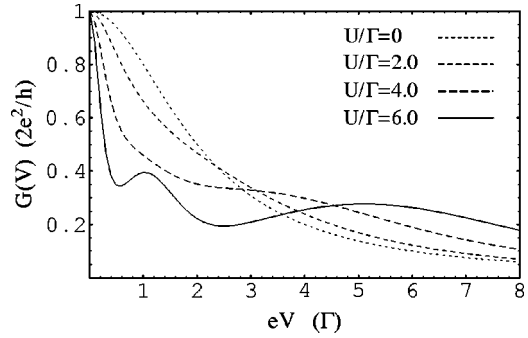

FIG. 5. The differential conductance in units of $2e^2/h$ for various values of U/Γ. The zero-bias peaks reach the unitary limit $2e^2/h$. For $U/\Gamma=6$, the anomalous peak is developed in $eV>k_BT_K$ in addition to the zero-bias peak.

the expression of the conductance, [Eq. (4)] as

$$G(V)=\frac{2e^2}{h}\pi\Gamma\left(\rho_\sigma(eV/2)+\int_{-eV/2}^{eV/2}\frac{\partial\rho_\sigma(\omega)}{\partial eV}d\omega\right)$$
$$\equiv G_1(V)+G_2(V). \tag{18}$$

As shown in Fig. 6, the first term, $G_1(V)$, decreases monotonically as V is increased. Concerning the second term $G_2(V)$ first we note that if the range of integration integrand is the entire frequency space, the integral should vanish due to the sum rule of the spectral weight. For $eV<k_BT_K$ the spectral weight shifts to higher frequencies, giving a negative contribution. When $eV\sim k_BT_K$ a considerable part of positive $\partial\rho_\sigma(\omega)/\partial eV$ enters in the integrand, thus giving a less negative contribution. Therefore we may conclude that the new peak appears when the bias voltage exceeds the Kondo energy.

V. DISCUSSIONS AND SUMMARY

Finally we discuss the possible relevance of the present study to the 0.7 conductance anomaly in QPCs.[15–17] It has been suggested that the Kondo effect plays a significant role as the origin of the 0.7 structure in QPCs because the structure is found when the unitary limit of $2e^2/h$ (Ref. 17) is approached with decreasing temperature. In view of the universal nature of the Kondo phenomena, it may be interesting

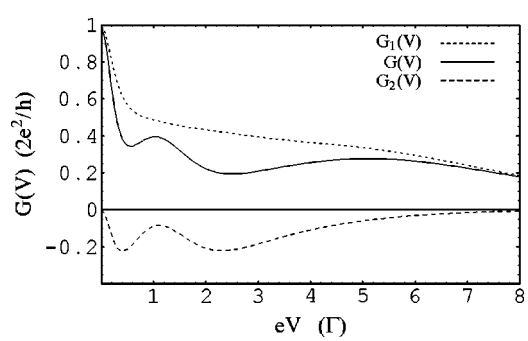

FIG. 6. The differential conductance for $U/\Gamma=6$. $G(V)$, is given by the sum of $G_1(V)$ and $G_2(V)$. The new peak originates in the behavior of $G_2(V)$.

to consider experimental results of the QPCs in light of the present results. Figure 3 of Ref. 16 or Fig. 1 of Ref. 17 show that at a gate voltage for which the zero-bias conductance reaches the unitary limit the conductance first drops with increasing bias voltage and then starts to increase again, leading to a second peak at finite voltage. The envelope made of these second peaks for different gate voltages forms the 0.8 plateau. As the temperature is increased the 0.8 plateau is extrapolated to the 0.7 structure in the zero-bias limit. In fact, Fig. 3(b) of Ref. 17 clearly demonstrates that a second peak appears when $eV > k_B T_K$. This result seems to support the new peak obtained in the present study.

However the peak-height obtained by the present study does not reach to 0.8, as seen in Fig. 5. This problem may be resolved in the future either by considering higher-order corrections or actual level schemes of the QPCs.

In summary we have studied the Kondo transport through a dot with a finite voltage by using perturbation theory in the Keldysh formalism. It is shown that the splitting of the Kondo resonance occurs when the bias voltage exceeds the Kondo temperature. As a result, the new peak in the differential conductance appears when the electron-electron correlation U is sufficiently strong. Finally, we have suggested that the present results are relevant also to the 0.7 conductance anomaly. Clearly further studies are necessary to elucidate the relation between the present analysis and the 0.7 anomaly in the QPCs.

ACKNOWLEDGMENTS

The authors would like to thank K. Kobayashi and A. Oguri for helpful discussions.

[1] T. K. Ng and P. A. Lee, Phys. Rev. Lett. **61**, 1768 (1988).
[2] L. I. Glazman and M. E. Raikh, Pis'ma. Zh. Éksp. Teor. Fiz. **47**, 378 (1988) [JETP Lett. **47**, 452 (1988)].
[3] D. Goldhaber-Gordon, H. Shtrikman, D. Mahalu, D. Abusch-Magder, U. Meirav, and M. A. Kastner, Nature (London) **391**, 156 (1998); D. Goldhaber-Gordon, J. Göres, M. A. Kastner, H. Shtrikman, D. Mahalu, and U. Meirav, Phys. Rev. Lett. **81**, 5225 (1998).
[4] S. M. Cronenwett, T. H. Oosterkamp, and L. P. Kouwenhoven, Science **281**, 540 (1998).
[5] W. G. van der Wiel, S. De Franceschi, T. Fujisawa, J. M. Elzerman, S. Tarucha, and L. P. Kouwenhoven, Science **289**, 2105 (2000).
[6] L. V. Keldysh, Zh. Éksp. Teor. Fiz. **47**, 1515 (1965) [Sov. Phys. JETP **20**, 1018 (1965)].
[7] S. Hershfield, J. H. Davies, and J. W. Wilkins, Phys. Rev. Lett. **67**, 3720 (1991); Phys. Rev. B **46**, 7046 (1992)
[8] Y. Meir, N. S. Wingreen and P. A. Lee, Phys. Rev. Lett. **70**, 2601 (1993); N. S. Wingreen and Y. Meir, Phys. Rev. B **49**, 11 040 (1994).
[9] K. Yosida and K. Yamada, Prog. Theor. Phys. Suppl. **46**, 244 (1970); Prog. Theor. Phys. **53**, 1286 (1975) K. Yamada, *ibid.* **53**, 970 (1975); *ibid.* **54**, 316 (1975).
[10] J. König, J. Schmid, H. Schoeller, and G. Schon, Phys. Rev. B **54**, 16 820 (1996).
[11] A. Rosch, J. Kroha, and P. Wölfle, Phys. Rev. Lett. **87**, 156802 (2001); cond-mat/0202404 (unpublished).
[12] Q. F. Sun and H. Guo, Phys. Rev. B **64**, 153306 (2001).
[13] E. Lebanon and A. Schiller, Phys. Rev. B **65**, 035308 (2002).
[14] S. De Franceschi, R. Hanson, W. G. van der Wiel, J. M. Elzerman, J. J. Wijpkema, T. Fujisawa, S. Tarucha, and L. P. Kouwenhoven, Phys. Rev. Lett. **89**, 156801 (2002).
[15] K. J. Thomas, J. T. Nicholls, M. Y. Simmons, M. Pepper, D. R. Mace, and D. A. Ritchie, Phys. Rev. Lett. **77**, 135 (1996).
[16] A. Kristensen, H. Bruus, A. E. Hansen, J. B. Jensen, P. E. Lindelof, C. J. Marckmann, J. Nygard, C. B. Sorensen, F. Beuscher, A. Forchel, and M. Michel, Phys. Rev. B **62**, 10 950 (2000).
[17] S. M. Cronenwett, H. J. Lynch, D. Goldhaber-Gordon, L. P. Kouwenhoven, C. M. Marcus, K. Hirose, N. S. Wingreen, and V. Umansky, Phys. Rev. Lett. **88**, 226805 (2002).
[18] V. Zlatić and B. Horvatić, Phys. Rev. B **28**, 6904 (1983); K. Ueda and W. Apel, J. Phys. C **16**, L849 (1983).
[19] A. Oguri, Phys. Rev. B **64**, 153305 (2001).